

# Nonlinear Analysis and Control of a Reaction Wheel-based 3D Inverted Pendulum

Michael Muehlebach, Gajamohan Mohanarajah, and Raffaello D'Andrea

**Abstract**—This paper presents the nonlinear analysis and control design of the Cubli, a reaction wheel-based 3D inverted pendulum. Using the concept of generalized momenta, the key properties of a reaction wheel-based 3D inverted pendulum are compared to the properties of a 1D case in order to come up with a relatively simple and intuitive nonlinear controller. Finally, the proposed controller is implemented on the Cubli, and the experimental results are presented.

## I. INTRODUCTION

This paper presents the nonlinear analysis and control of the Cubli shown in Figure 1. The Cubli is a cube of 150 mm side length with three reaction wheels mounted orthogonally to each other. Compared to other 3D inverted pendulum test beds [1] and [2], the Cubli has two unique features. One is its relatively small footprint (hence the name Cubli, which is derived from the Swiss German diminutive for “cube”). The other feature is its ability to jump up from a resting position without any external support, by suddenly braking its reaction wheels rotating at high angular velocities. While the concept of jumping up is covered in [3], and a linear controller is presented in [4], this paper focuses on the analysis of the nonlinear model and nonlinear control strategies.

In contrary to the works presented in [5] and [6], this paper approaches the controller design from a purely mechanical point of view. Fundamental mechanical properties of the Cubli are exploited to come up with simple and intuitive derivations with physical insights ([5]: 1D, reaction wheel, feedback linearization; [6]: 3D, proof mass, linear controller, local stability). The resulting smooth, asymptotically stable control law provides a relatively simple tuning strategy based on four intuitive parameters, thus making the control law suitable for practical implementations.

The remainder of this paper is structured as follows: A brief nonlinear analysis and control of the reaction wheel-based 1D inverted pendulum is first presented in Section II. Next, the nonlinear system dynamics is derived from first principles in Section III, which is followed by a detailed analysis and control design in Sections IV and V, respectively. Finally, experimental results are presented in Section VI and conclusions are made in Section VII.

## II. ANALYSIS AND CONTROL OF A 1D INVERTED PENDULUM

This section presents the analysis and nonlinear control strategy for a 1D reaction wheel-based inverted pendulum.

The authors are with the Institute for Dynamic Systems and Control, Swiss Federal Institute of Technology Zürich, Switzerland. The contact author is M. Gajamohan, e-mail: gajan@ethz.ch.

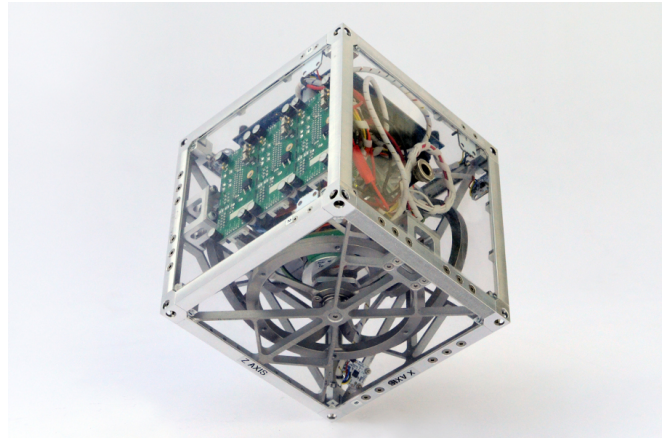


Fig. 1. Cubli balancing on a corner. In the current version, the Cubli (controller) must be initialized while holding the Cubli near the equilibrium position.

Due to the similarity of some key properties in both the 1D and 3D cases, this section sets the stage for the analysis of the 3D inverted pendulum in the later sections.

### A. Modelling

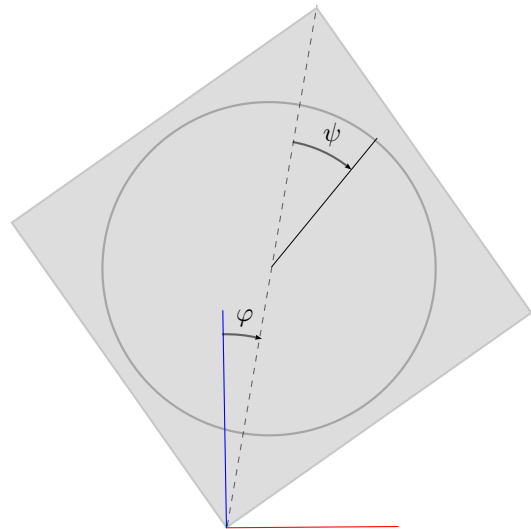


Fig. 2. A schematic diagram of a reaction wheel based 1D inverted pendulum. This can be realized by putting the Cubli on one of its edges.

Let  $\varphi$  and  $\psi$  describe the positions of the 1D inverted pendulum as shown in Figure 2. Next, let  $\Theta_w$  denote the reaction wheel’s moment of inertia,  $\Theta_0$  denote the system’s total moment of inertia around the pivot point in the body

fixed coordinate frame, and  $m_{tot}$  and  $l$  represent the total mass and distance between the pivot point to the center of gravity of the whole system.

The Lagrangian [7] of the system is given by:

$$\mathcal{L} = \frac{1}{2}\hat{\Theta}_0\dot{\varphi}^2 + \frac{1}{2}\Theta_w(\dot{\varphi} + \dot{\psi})^2 - mg \cos \varphi, \quad (1)$$

where  $\hat{\Theta}_0 = \Theta_0 - \Theta_w > 0$ ,  $m = m_{tot}l$  and  $g$  is the constant gravitational acceleration. The generalized momenta are defined by

$$p_\varphi := \frac{\partial \mathcal{L}}{\partial \dot{\varphi}} = \Theta_0\dot{\varphi} + \Theta_w\dot{\psi}, \quad (2)$$

$$p_\psi := \frac{\partial \mathcal{L}}{\partial \dot{\psi}} = \Theta_w(\dot{\varphi} + \dot{\psi}). \quad (3)$$

Let  $T$  denote the torque applied to the reaction wheel by the motor. Now, the equations of motion can be derived using the Euler-Lagrange equations with the torque  $T$  as a non-potential force. This yields

$$\dot{p}_\varphi = \frac{\partial \mathcal{L}}{\partial \varphi} = mg \sin \varphi, \quad (4)$$

$$\dot{p}_\psi = \frac{\partial \mathcal{L}}{\partial \psi} + T = T. \quad (5)$$

Note that the introduction of the generalized momenta in (2) and (3) leads to a simplified representation of the system, where (4) resembles an inverted pendulum augmented by an integrator in (5).

Since the actual position of the reaction wheel is not of interest, we introduce  $x := (\varphi, p_\varphi, p_\psi)$  to represent the reduced set of states and describe the dynamics of the mechanical system as follows:

$$\dot{x} = \begin{pmatrix} \dot{\varphi} \\ \dot{p}_\varphi \\ \dot{p}_\psi \end{pmatrix} = f(x, T) = \begin{pmatrix} \hat{\Theta}_0^{-1}(p_\varphi - p_\psi) \\ mg \sin \varphi \\ T \end{pmatrix}. \quad (6)$$

## B. Analysis

1) *State Space*: For the subsequent analysis the state space is defined as  $\mathcal{X} = \{x \mid \varphi \in (-\pi, \pi], p_\varphi \in \mathbb{R}, p_\psi \in \mathbb{R}\}$ .

2) *Equilibria*: The equilibria of the system are given by  $\mathcal{E} = \{(x, T) \in \mathcal{X} \times \mathbb{R} \mid f(x, T) = 0\}$ . Evaluating  $\dot{p}_\varphi = \dot{p}_\psi = \dot{\varphi} = 0$  gives the following equilibria:

$$\mathcal{E}_1 = \{(x, T) \in \mathcal{X} \times \mathbb{R} \mid \varphi = 0, p_\varphi = p_\psi, T = 0\}, \quad (7)$$

$$\mathcal{E}_2 = \{(x, T) \in \mathcal{X} \times \mathbb{R} \mid \varphi = \pi, p_\varphi = p_\psi, T = 0\}. \quad (8)$$

Each equilibrium is a closed invariant set with a constant  $p_\psi$  which may be non-zero. Mechanically, this means that the pendulum may be at rest in an upright position while its reaction wheel rotates at a constant angular velocity. Further linear analysis reveals that the upright equilibria  $\mathcal{E}_1$  is unstable, while the hanging equilibria  $\mathcal{E}_2$  is stable in the sense of Lyapunov.

## C. Control Design

The goal of the controller is to drive the inverted pendulum towards the upright position  $\varphi = 0$  and to bring the angular velocity of the reaction wheel  $\dot{\psi}$  to zero, specifically

$$\lim_{t \rightarrow \infty} x = 0. \quad (9)$$

Now, consider the following feedback control law

$$u(\varphi, p_\varphi, p_\psi) = k_1 mg \sin \varphi + k_2 p_\varphi - k_3 p_\psi, \quad (10)$$

where

$$k_1 = 1 + \alpha \hat{\Theta}_0 + \frac{\beta \gamma}{mg} + \delta,$$

$$k_2 = \frac{\beta}{\hat{\Theta}_0} \cos \varphi + \gamma(1 + \alpha \hat{\Theta}_0),$$

$$k_3 = \frac{\beta}{\hat{\Theta}_0} \cos \varphi + \gamma \quad \text{and}$$

$$\alpha, \beta, \gamma, \delta > 0.$$

*Theorem 2.1*: The control law  $T = u(\varphi, p_\varphi, p_\psi)$  given in (10) makes the equilibrium point  $x = 0$  stable and asymptotically stable on the domain  $\mathcal{X}^- = \mathcal{X} \setminus \{\varphi = \pi, p_\varphi = 0, p_\psi = 0\}$ .

*Proof*: Consider the following Lyapunov candidate function  $V : x \in \mathcal{X} \rightarrow \mathbb{R}$ ,

$$V(x) = \frac{1}{2}\alpha p_\varphi^2 + mg(1 - \cos \varphi) + \frac{1}{2\delta \hat{\Theta}_0} z^2, \quad (11)$$

where  $z = z(x) = p_\varphi(1 + \alpha \hat{\Theta}_0) + \beta \sin \varphi - p_\psi$ . There exists the class  $\mathcal{K}_\infty^1$  function  $a(x) := \epsilon x^2$  with  $\epsilon < \min\{\frac{2mg}{\pi^2}, \frac{\alpha}{2}, \frac{1}{2\delta \hat{\Theta}_0}\}$  such that  $V(x) \geq a(\|(p_\varphi, \varphi, z)\|_2) \forall x \in \mathcal{X}$  and  $V(0) = 0$ . Hence,  $V(x)$  is positive definite and a valid Lyapunov candidate.

The time derivative of the above Lyapunov candidate function along the closed loop trajectory is given by

$$\begin{aligned} \dot{V}(x) &= \frac{mg}{\hat{\Theta}_0} (z - \beta \sin \varphi) \sin \varphi + \frac{1}{\delta \hat{\Theta}_0} z \dot{z} \\ &= -\frac{mg}{\hat{\Theta}_0} \beta \sin^2 \varphi - \frac{\gamma}{\delta \hat{\Theta}_0} z^2 \leq 0, \quad \forall x \in \mathcal{X}. \end{aligned}$$

Since  $\dot{V}(x) \leq 0 \forall x \in \mathcal{X}$ , we conclude from Lyapunov's stability theorem that the point  $x = 0$  is stable.

Now, to prove asymptotic stability of  $x = 0$  in  $\mathcal{X}^-$ , let us define the set

$$\mathcal{R} = \{x \in \mathcal{X}^- \mid \dot{V}(x) = 0\}.$$

Consider trajectories  $x(t)$  inside an invariant set of  $\mathcal{R}$ . Clearly, they must fulfill  $\varphi = 0$ ,  $z = 0$  and the system dynamics (6). This implies  $x(t) \equiv 0$  and therefore the largest invariant set in  $\mathcal{R}$  is  $x = 0$ . Now, by Krasovskii-LaSalle principle [9] (Theorem 4.4) it follows that, for any trajectory  $x(t)$ ,

$$\lim_{t \rightarrow \infty} x(t) = 0, \quad x(0) \in \mathcal{X}^-.$$

For a similar control design and stability proof of the 1D reaction wheel-based inverted pendulum, see [10].

<sup>1</sup>A function  $a : \mathbb{R} \rightarrow \mathbb{R}_0^+$  is of class  $\mathcal{K}_\infty$ , if it is strictly increasing and  $a(r = 0) = 0$ ,  $\lim_{r \rightarrow \infty} a(r) \rightarrow \infty$ , see [8].

#### D. Remarks

1) *Interpretation of the Lyapunov function (11):* The Lyapunov function (11) can be found by a standard backstepping approach [9], [10]. If the reaction wheel dynamics are neglected and  $p_\psi$  is assumed to be the control input, the function  $\tilde{V}(\varphi, p_\varphi) = \frac{1}{2}\alpha p_\varphi^2 + mg(1 - \cos \varphi)$  is a valid Lyapunov function candidate. Requiring  $\dot{\tilde{V}} \leq 0$  along trajectories would imply  $p_\psi = p_\varphi(1 + \alpha\hat{\Theta}_0) + \beta \sin \varphi$ , i.e.  $z = 0$ . This leads to the interpretation that  $z$  penalizes the deviation from the control law that would be applied to the system when neglecting wheel dynamics. Hence, decreasing the tuning parameter  $\delta$  leads to a more aggressive controller that prioritizes the tilt over the wheel velocity.

2) *Extension of the controller (10):* The Lyapunov function (11) can be augmented by an additional integrator state,

$$\hat{V}(x) = V(x) + \frac{\nu}{2\delta\hat{\Theta}_0} z_{int}^2,$$

where  $z_{int}(t) = z_0 + \int_0^t z(\tau)d\tau$ . As a consequence, the controller (10) must be extended with  $z_{int}$ ,  $\hat{u} = u + \nu z_{int}$  in order to provide stability of the upright equilibrium. This may also be important for practical implementation since it accounts for modelling errors.

3) *Interpretation of the control law (10):* The control law given in (10) can be rewritten as

$$u = \frac{\beta}{mg} \ddot{p}_\varphi + k_1 \dot{p}_\varphi + \gamma(1 + \alpha\hat{\Theta}_0)p_\varphi - \gamma p_\psi,$$

where

$$p_\psi = u_0 + \int_0^t u(\tau)d\tau.$$

This is nothing but a linear controller composed of a proportional, (double) differential, and integral parts. Furthermore  $\gamma$  can be interpreted as the integrator weight.

### III. SYSTEM DYNAMICS OF THE REACTION WHEEL-BASED 3D INVERTED PENDULUM

Let  $\Theta_0$  denote the total moment of inertia of the full Cubli around the pivot point  $O$  (see Figure 3),  $\Theta_{wi}$ ,  $i = 1, 2, 3$  denote the moment of inertia of each reaction wheel (in the direction of the corresponding rotation axis) and define  $\Theta_w := \text{diag}(\Theta_{w1}, \Theta_{w2}, \Theta_{w3})$ ,  $\hat{\Theta}_0 := \Theta_0 - \Theta_w$ . Next, let  $\tilde{m}$  denote the position vector from the pivot point to the center of gravity multiplied by the total mass and  $\vec{g}$  denote the gravity vector. The projection of a tensor onto a particular coordinate frame is denoted by a preceding superscript, i.e.  ${}^B\Theta_0 \in \mathbb{R}^{3 \times 3}$ ,  ${}^B(\tilde{m}) = {}^Bm \in \mathbb{R}^3$ . The arrow notation is used to emphasize that a vector (and tensor) should be a priori thought of as a linear object in a normed vector space detached from its coordinate representation with respect to a particular coordinate frame. Since the body fixed coordinate frame  $\{B\}$  is the most commonly projected coordinate frame, we usually remove its preceding superscript for the sake of simplicity. Note further that  ${}^B\hat{\Theta}_0 = \hat{\Theta}_0 \in \mathbb{R}^{3 \times 3}$  is positive definite.

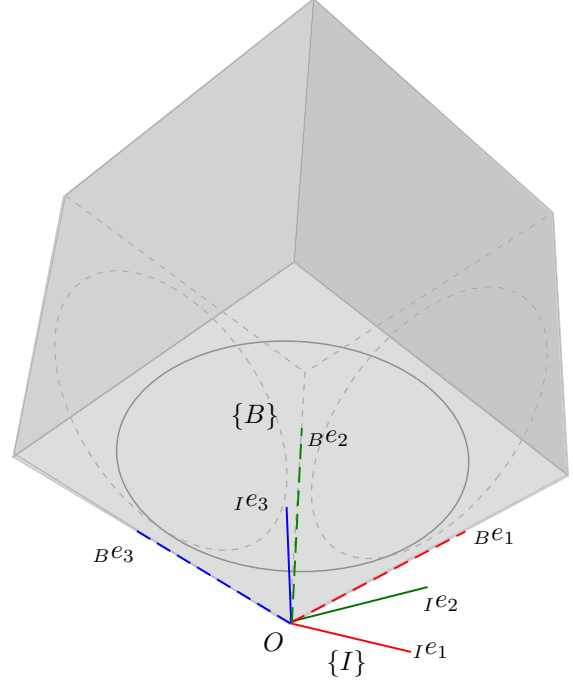


Fig. 3. Cubli balancing on the corner.  $B e_*$  and  $I e_*$  denote the principle axis of the body fixed frame  $\{B\}$  and inertial frame  $\{I\}$ . The pivot point  $O$  is the common origin of coordinate frames  $\{I\}$  and  $\{B\}$ .

The Lagrangian of the system is given by

$$\mathcal{L}(\omega_h, g, \omega_w, \phi) = \frac{1}{2} \omega_h^T \hat{\Theta}_0 \omega_h + \frac{1}{2} (\omega_h + \omega_w)^T \Theta_w (\omega_h + \omega_w) + m^T g, \quad (12)$$

where  ${}^B(\vec{\omega}_h) = \omega_h \in \mathbb{R}^3$  denotes the body angular velocity and  ${}^B(\vec{\omega}_w) = \omega_w \in \mathbb{R}^3$  denotes the reaction wheel angular velocity. The components of  $T \in \mathbb{R}^3$  contain the torques as applied to the reaction wheels. In the body fixed coordinate frame, the vector  $m$  is constant whereas the time derivative of  $g$  is given by  ${}^B(\dot{g}) = 0 = \dot{g} + \omega_h \times g = \dot{g} + \tilde{\omega}_h g$ . The tilde operator applied to the vector  $v \in \mathbb{R}^3$ , i.e.  $\tilde{v}$  denotes the skew symmetric matrix for which  $\tilde{v}a = v \times a$  holds  $\forall a \in \mathbb{R}^3$ .

Introducing the generalized momenta

$$p_{\omega_h} =: \frac{\partial \mathcal{L}}{\partial \omega_h} = \Theta_0 \omega_h + \Theta_w \omega_w, \quad (13)$$

$$p_{\omega_w} =: \frac{\partial \mathcal{L}}{\partial \omega_w} = \Theta_w (\omega_h + \omega_w) \quad (14)$$

results in the equations of motion given by

$$\dot{g} = -\tilde{\omega}_h g, \quad (15)$$

$$\dot{p}_{\omega_h} = -\tilde{\omega}_h p_{\omega_h} + \tilde{m} g, \quad (16)$$

$$\dot{p}_{\omega_w} = T. \quad (17)$$

Note that there are several ways of deriving the equations of motion; for example in [4] the concept of virtual power has been used. A derivation using the Lagrangian formalism is shown in the appendix <sup>2</sup> and highlights the similarities

<sup>2</sup>[http://www.idsc.ethz.ch/Research\\_DAndrea/Cubli/cubliCDC13-appendix.pdf](http://www.idsc.ethz.ch/Research_DAndrea/Cubli/cubliCDC13-appendix.pdf)

between the 1D and 3D case. The Lagrangian formalism also motivates the introduction of the generalized momenta.

Now, using  $\dot{\vec{v}} = \dot{v} + \omega_h \times v$ , the time derivative of a vector in a rotating coordinate frame, (15)-(17) can be further simplified to

$$\dot{\vec{g}} = 0, \quad (18)$$

$$\dot{p}_{\omega_h} = \vec{m} \times \vec{g}, \quad (19)$$

$$\dot{p}_{\omega_w} = T. \quad (20)$$

This highlights, in particular, the similarity between the 1D and 3D inverted pendula. Since the norm of a vector is independent of its representation in a coordinate frame, the 2-norm of the impulse change is given by  $\|\dot{p}_{\omega_h}\|_2 = \|\vec{m}\|_2 \|\vec{g}\|_2 \sin \phi$ . In this case,  $\phi$  denotes the angle between the vectors  $\vec{m}$  and  $\vec{g}$ . Additionally, as in the 1D case,  $p_{\omega_w}$  is the integral of the applied torque  $T$ .

#### IV. ANALYSIS

##### A. Conservation of Angular Momentum

From (19) it follows that the rate of change of  $\vec{p}_{\omega_h}$  lies always orthogonal to  $\vec{m}$  and  $\vec{g}$ . Since  $\vec{g}$  is constant,  $\vec{p}_{\omega_h}$  will never change its component in direction  $\vec{g}$  during the whole trajectory. Expressed in Cubli's body fixed coordinate frame, it can be written as  $\frac{d}{dt}(p_{\omega_h}^T g) \equiv 0$  and this is nothing but the conservation of angular momentum around the axis  $\vec{g}$ .

This has a very important consequence for the control design: Independent of the control input applied, the momentum around  $\vec{g}$  is conserved and, depending on the initial condition, it may be impossible to bring the system to rest.

##### B. State Space

Since the subsequent analysis and control will be carried out in the fixed body coordinate frame, the state space is defined by the set  $\mathcal{X} = \{x = (g, p_{\omega_h}, p_{\omega_w}) \in \mathbb{R}^9 \mid \|g\|_2 = 9.81\}$ . Note that  $\omega_h = \hat{\Theta}_0^{-1}(p_{\omega_h} - p_{\omega_w})$ .

##### C. Equilibria

The procedure is identical to the one presented in subsection II-B.2. As can be seen from (19), the condition  $\dot{p}_{\omega_h} = 0$  is fulfilled only if  $m \parallel g$ , i.e.,  $g = \pm \frac{m}{\|m\|_2} \|g\|_2$ . From (20) it follows that  $p_{\omega_w} = \text{const}$ ,  $T = 0$ . Using (15) and (16) leads to  $\omega_h = \hat{\Theta}_0^{-1}(p_{\omega_h} - p_{\omega_w}) \parallel g$  and  $p_{\omega_h} \parallel g$ , which corresponds exactly to the conserved part of  $p_{\omega_h}$ . Combining everything together results in the following equilibria

$$\mathcal{E}_1 = \{(x, T) \in \mathcal{X} \times \mathbb{R}^3 \mid g^T m = -\|g\|_2 \|m\|_2,$$

$$p_{\omega_h} \parallel m, \hat{\Theta}_0^{-1}(p_{\omega_h} - p_{\omega_w}) \parallel m, T = 0\},$$

$$\mathcal{E}_2 = \{(x, T) \in \mathcal{X} \times \mathbb{R}^3 \mid g^T m = \|g\|_2 \|m\|_2,$$

$$p_{\omega_h} \parallel m, \hat{\Theta}_0^{-1}(p_{\omega_h} - p_{\omega_w}) \parallel m, T = 0\}.$$

Linearization reveals that the upright equilibria  $\mathcal{E}_1$  is unstable, while the hanging equilibria  $\mathcal{E}_2$  is stable in the sense of Lyapunov.

#### V. NONLINEAR CONTROL OF THE REACTION WHEEL-BASED 3D INVERTED PENDULUM

Let us first define the control objective. Since the angular momentum  $\vec{p}_{\omega_h}$  is conserved in the direction of  $\vec{g}$ , the controller may only bring the component of  $\vec{p}_{\omega_h}$  that is orthogonal to  $\vec{g}$  to zero. Hence it is convenient to split the vector  $\vec{p}_{\omega_h}$  into two parts: one in the direction of  $\vec{g}$ , and one orthogonal to it, i.e.

$$\vec{p}_{\omega_h} = \vec{p}_{\omega_h}^\perp + \vec{p}_{\omega_h}^g \quad \text{and} \quad \vec{p}_{\omega_h}^g = (\vec{p}_{\omega_h}^T \vec{g}) \frac{\vec{g}}{\|\vec{g}\|_2^2}.$$

From (19) and the conservation of angular momentum, it follows directly that

$${}^B(\dot{\vec{p}}_{\omega_h}^\perp) = \dot{p}_{\omega_h}^\perp + \tilde{\omega}_h p_{\omega_h}^\perp = \tilde{m}g. \quad (21)$$

Another reasonable addition to the control objective is the asymptotic convergence of the angular velocity of the Cubli,  $\omega_h$ , to zero. Consequently, the control objective can be formulated as driving the system to the closed invariant set  $\mathcal{T} = \{x \in \mathcal{X} \mid g^T m = -\|g\|_2 \|m\|_2, \omega_h = \hat{\Theta}_0^{-1}(p_{\omega_h} - p_{\omega_w}) = 0, p_{\omega_h}^\perp = 0\}$ .

In order to prove asymptotic stability, the hanging equilibrium must be excluded (as will become clear later). This can be done by introducing the set  $\mathcal{X}^- = \mathcal{X} \setminus x^-$ , where  $x^-$  denotes the hanging equilibrium with  $\omega_h = 0$ :

$$x^- = \{x \in \mathcal{X} \mid g = \frac{\|g\|_2}{\|m\|_2} m, p_{\omega_h}^\perp = 0, p_{\omega_h} = p_{\omega_w}\}.$$

Next, consider the controller

$$u = K_1 \tilde{m}g + K_2 \omega_h + K_3 p_{\omega_h} - K_4 p_{\omega_w}, \quad (22)$$

where

$$K_1 = (1 + \beta\gamma + \delta)I + \alpha \hat{\Theta}_0,$$

$$K_2 = \alpha \hat{\Theta}_0 \tilde{p}_{\omega_h}^\perp + \beta \tilde{m} \tilde{g} + \tilde{p}_{\omega_h},$$

$$K_3 = \gamma(I + \alpha \hat{\Theta}_0 (I - \frac{gg^T}{\|g\|_2^2})),$$

$$K_4 = \gamma I, \quad \alpha, \beta, \gamma, \delta > 0,$$

and  $I \in \mathbb{R}^{3 \times 3}$  is the identity matrix.

*Theorem 5.1:* The controller given in (22) makes the closed invariant set  $\mathcal{T}$  of the system defined by (18)-(20) stable and asymptotically stable on  $x \in \mathcal{X}^-$ .

*Proof:* Consider the following Lyapunov candidate function  $V : \mathcal{X} \rightarrow \mathbb{R}$ ,

$$V(x) = \frac{1}{2} \alpha p_{\omega_h}^\perp{}^T p_{\omega_h}^\perp + m^T g + \|m\|_2 \|g\|_2 + \frac{1}{2\delta} z^T \hat{\Theta}_0^{-1} z, \quad (23)$$

with  $z = z(x) = \alpha \hat{\Theta}_0 p_{\omega_h}^\perp + p_{\omega_h} + \beta \tilde{m}g - p_{\omega_w}$ .

Then the  $\mathcal{K}_\infty$  function  $a(x) := \epsilon x^2$ , with  $\epsilon < \min\{\frac{2}{\pi^2} \|m\|_2 \|g\|_2, \frac{1}{2\delta \|\hat{\Theta}_0\|_2}, \frac{\alpha}{2}\}$  is such that  $V(x) \geq a(\|(p_{\omega_h}^\perp, p_{\omega_w}, z)\|_2)$ ,  $\forall x \in \mathcal{X}$ . Furthermore  $V(x = x_0) = 0$  implies  $x = x_0$ , where  $x_0 \in \mathcal{T}$ . Therefore  $V$  is a positive definite function and a valid Lyapunov candidate.

Next,  $\dot{V}$  is evaluated along trajectories of the closed loop system:

$$\begin{aligned}\dot{V}(x) &= \alpha p_{\omega_h}^{\perp T} \dot{p}_{\omega_h}^{\perp} + m^T \dot{g} + \frac{1}{\delta} z^T \hat{\Theta}_0^{-1} \dot{z} \\ &= m^T \tilde{g} \hat{\Theta}_0^{-1} (\beta \tilde{g} m + z) + \frac{1}{\delta} z^T \hat{\Theta}_0^{-1} \dot{z} \\ &= -\beta (\tilde{g} m)^T \hat{\Theta}_0^{-1} (\tilde{g} m) + z^T \hat{\Theta}_0^{-1} (\tilde{m} g + \frac{1}{\delta} \dot{z}) \\ &= -\beta (\tilde{g} m)^T \hat{\Theta}_0^{-1} (\tilde{g} m) - \frac{\gamma}{\delta} z^T \hat{\Theta}_0^{-1} z \leq 0, \forall x \in \mathcal{X}.\end{aligned}$$

Since  $\dot{V}(x) \leq 0 \forall x \in \mathcal{X}$ , we conclude from Lyapunov's stability theorem that the point  $x_0 \in \mathcal{T}$  is stable.

To prove asymptotic stability of the set  $\mathcal{T}$  in  $\mathcal{X}^-$  define the set  $\mathcal{R} := \{x \in \mathcal{X}^- \mid \dot{V}(x) = 0\}$ . The condition  $\dot{V}(x) = 0$  leads immediately to  $z = 0$ ,  $m \parallel g$ , such that  $\mathcal{R}$  can be rewritten as  $\mathcal{R} = \{x \in \mathcal{X}^- \mid m \parallel g, p_{\omega_w} = \alpha \hat{\Theta}_0 p_{\omega_h}^{\perp} + p_{\omega_h}\}$ . Now, let us consider the system dynamics of a trajectory inside an invariant set contained in  $\mathcal{R}$ . This gives

$$\begin{aligned}g \parallel m \Rightarrow g &= -\frac{m}{\|m\|_2} \|g\|_2 \Rightarrow \dot{g} = 0 \\ \Rightarrow \omega_h \parallel g \quad \therefore \dot{g} &= -\tilde{\omega}_h g\end{aligned}\quad (24)$$

$$\begin{aligned}g \parallel m, z = 0 \Rightarrow \omega_h &= \alpha p_{\omega_h}^{\perp} \\ \Rightarrow \omega_h \parallel p_{\omega_h}^{\perp}\end{aligned}\quad (25)$$

However, since  $p_{\omega_h}^{\perp} \perp g$  by definition, (24) and (25) imply  $\omega_h = 0$  and  $p_{\omega_h}^{\perp} = 0$ . This shows that  $\mathcal{T}$  is the largest invariant subset of  $\mathcal{R}$ . Now, by Krasovskii-LaSalle principle [9] (Theorem 4.4), it follows that, for any trajectory  $x(t)$ ,

$$\lim_{t \rightarrow \infty} x(t) = x_f, \quad x(0) \in \mathcal{X}^-, \quad x_f \in \mathcal{T}.$$

■

#### A. Remarks

1) *Interpretation of the Lyapunov function (23)*: Similar to the 1D case, the Lyapunov function (23) can be found via a two-step backstepping approach. The reduced Lyapunov function  $\tilde{V}(x) = \frac{1}{2} \alpha p_{\omega_h}^{\perp T} p_{\omega_h}^{\perp} + m^T g + \|m\|_2 \|g\|_2$  can be used to demonstrate stability for  $p_{\omega_w} = \alpha \hat{\Theta}_0 p_{\omega_h}^{\perp} + p_{\omega_h} + \beta \tilde{m} g$ , i.e.  $z = 0$ . Therefore  $z$  can again be interpreted as penalty term, see Section II-D.

2) *Extension of the controller (22)*: As in the 1D case, the Lyapunov function (23) can be extended with an additional state,

$$\hat{V}(x) = V(x) + \frac{\nu}{2\delta} z_{int}^T \hat{\Theta}_0^{-1} z_{int}, \quad z_{int}(t) = z_0 + \int_0^t z(\tau) d\tau.$$

Straightforward derivation shows that the resulting controller must be augmented by  $z_{int}$ , i.e.  $\hat{u} = u + \nu z_{int}$ . Integral control is useful in practice to prevent steady state deviations caused by modelling errors.

#### B. Interpretation of the control law (22)

Rewriting (22) yields

$$\begin{aligned}u &= \dot{p}_{\omega_h} + \gamma p_{\omega_h} + \alpha \hat{\Theta}_0 (\dot{p}_{\omega_h}^{\perp} + \gamma p_{\omega_h}^{\perp}) + \\ &\quad \tilde{m} (\beta \dot{g} + (\delta + \gamma \beta) g) - \gamma p_{\omega_w},\end{aligned}\quad (26)$$

where

$$p_{\omega_w} = u_0 + \int_0^t u(\tau) d\tau.$$

Therefore the controller given in (22) is a linear PID controller in the variables  $p_{\omega_w}, p_{\omega_w}^{\perp}$  and  $g$ . The nonlinearity of the controller lies in the projection of  $p_{\omega_h}$  into  $p_{\omega_h}^{\perp}$  and  $p_{\omega_h}^g$ , and the computation of the  $g$ -vector from the quaternion based position estimate. Now, for small inclination angles of the body, the above nonlinear effects can be neglected to give a linearized controller that has a similar performance to the proposed nonlinear controller.

#### C. Offset-Correction Filter

Although the Cubli is stabilized in upright position, the desired equilibrium ( $x \in \mathcal{T}$ ) may not be reached in practice. This is due to modelling errors,  $\Delta m$  of the parameter  $m$ . Denote  $\hat{m} = m + \Delta m$ , the wrong estimate of the parameter  $m$ . Since the Cubli cannot reach an equilibrium position other than  $m \parallel g$  (see Section IV-C), the modelling errors can be reduced by projecting  $\hat{m}$  on  $g$ . This adaptation can be made iteratively, but must be carried out very slowly, in order to keep the upright equilibrium stable. Since the controller is implemented in discrete time, this leads to the following heuristic algorithm:

$$\hat{m}_0 = \hat{m}, \quad (27)$$

$$\hat{m}_{k+1} = \mu \frac{\hat{m}_k^T g}{\|g\|_2} \frac{g}{\|g\|_2} + (1 - \mu) \hat{m}_k, \quad (28)$$

$$\hat{m}_{k+1} = \hat{m}_{k+1} \frac{\|\hat{m}_k\|_2}{\|\hat{m}_{k+1}\|_2}, \quad (29)$$

where  $\mu$  ( $\mu \ll 1$ ) represents the time constant of the adaptation. Note that (29) is required to ensure that the magnitude of  $\hat{m}$  is not affected.

## VI. EXPERIMENTAL RESULTS

This section presents disturbance rejection measurements of the proposed controller. The controller given in (22) is implemented on the Cubli with a sampling time of  $T_s = 50$  ms along with the algorithm proposed in [2] for state estimation.

Figures 4 and 5 show disturbance rejection plots of the proposed controller. A disturbance of roughly 0.1 Nm was applied for 60 ms on each of the reaction wheels simultaneously. The control input shown in Figure 6, where the controller reaches the steady state control input in less than 0.3 s. Finally, the controller attained a root mean square (RMS) inclination error of less than  $0.025^\circ$  at steady state. For small inclination angles, the linearized counterpart of the proposed controller also gave a similar performance. Note that the experimental setup did not allow large inclinations due to the saturation of the motor torques (80 [mNm]).

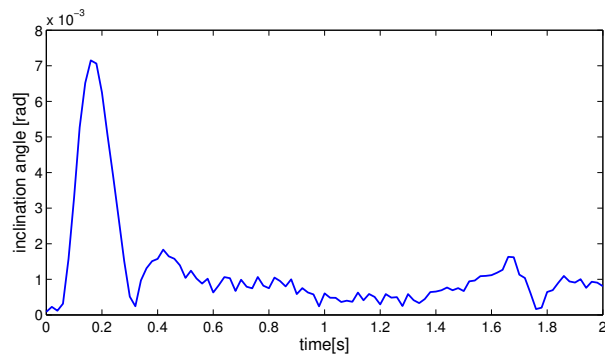


Fig. 4. Disturbance rejection measurement. Depicted is the resulting inclination angle of the nonlinear controller. In this case an asymmetric disturbance of roughly 0.1[Nm] is applied simultaneously on two reaction wheels.

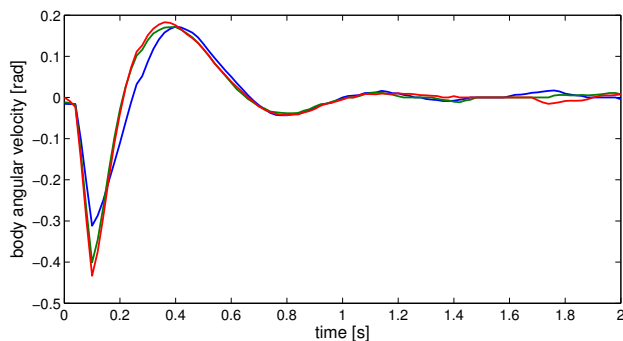


Fig. 5. Disturbance rejection measurement. Depicted is the resulting body angle velocity,  $\omega_h$  of the nonlinear controller. The different colors depict the different vector components of  $\omega_h$ . In this case an asymmetric disturbance of roughly 0.1[Nm] is applied simultaneously on two reaction wheels.

## VII. CONCLUSION

This paper represents a further step in the development of the Cubli: a 3D inverted pendulum with a relatively small footprint. By using the concept of generalized momenta, the dynamics of the reaction wheel-based 3D inverted pendulum were put in relation to the 1D case. The key properties of the pendulum system were analyzed and a controller was proposed, which was shown to asymptotically stabilize the upright equilibrium. Finally, the controller was implemented on the Cubli, tuned using its intuitive parameters, and its performance was evaluated.

## ACKNOWLEDGEMENTS

The authors would like to express their gratitude towards Igor Thommen, Corzillius Marc-Andrea, Hans Ulrich Honegger, Alex Braun, Tobias Widmer, Felix Berkenkamp, and Sonja Segmueller for their significant contribution to the mechanical and electronic design of the Cubli.

## REFERENCES

[1] D. Bernstein, N. McClamroch, and A. Bloch, "Development of air spindle and triaxial air bearing testbeds for spacecraft dynamics and control experiments," in *American Control Conference*, 2001, pp. 3967–3972.

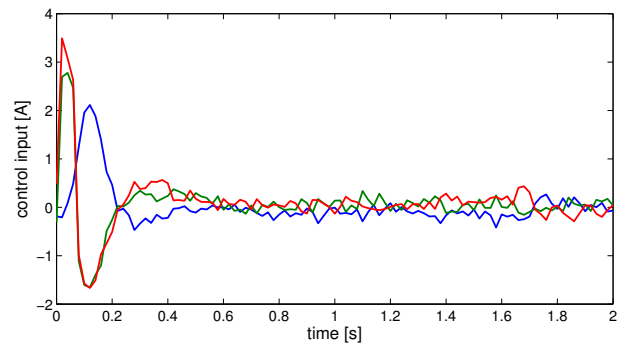


Fig. 6. Disturbance rejection measurement. Depicted is the resulting control input of the nonlinear controller. The different colors depict the different vector components of  $u \propto T$ . In this case an asymmetric disturbance of roughly 0.1[Nm] is applied simultaneously on two reaction wheels.

- [2] S. Trimpe and R. D'Andrea, "Accelerometer-based tilt estimation of a rigid body with only rotational degrees of freedom," in *IEEE International Conference on Robotics and Automation (ICRA)*, 2010, pp. 2630–2636.
- [3] M. Gajamohan, M. Merz, I. Thommen, and R. D'Andrea, "The Cubli: A cube that can jump up and balance," in *IEEE/RSJ International Conference on Intelligent Robots and Systems (IROS)*, 2012, pp. 3722–3727.
- [4] M. Gajamohan, M. Muehlebach, T. Widmer, and R. DAndrea, "The Cubli: A reaction wheel based 3D inverted pendulum," in *Proceedings of the European Control Conference*, 2013.
- [5] S. Cho and N. McClamroch, "Feedback control of triaxial attitude control testbed actuated by two proof mass devices," in *Proceedings of the 41st IEEE Conference on Decision and Control*, 2002, pp. 498–503.
- [6] M. W. Spong, P. Corke, and R. Lozano, "Brief nonlinear control of the reaction wheel pendulum," *Automatica*, pp. 1845–1851, 2001.
- [7] L. Cornelius, *The variational principles of mechanics*, 4th ed. University of Toronto Press Toronto, 1970.
- [8] H. Khalil, *Nonlinear Systems, Section 4.4 - Definition 4.3*. Upper Saddle River, New Jersey: Prentice Hall, 1996.
- [9] —, *Nonlinear Systems*. Upper Saddle River, New Jersey: Prentice Hall, 1996.
- [10] R. Olfati-Saber, "Nonlinear control of underactuated mechanical systems with application to robotics and aerospace vehicles," Ph.D. dissertation, Massachusetts Institute of Technology, 2000, <http://engineering.dartmouth.edu/~olfati/papers/phdthesis.pdf> visited on 2013-07-30.